

Dynamics of Water Filaments in Disordered Environments

Marek Orzechowski and Markus Meuwly*

Department of Chemistry, University of Basel, Klingelbergstrasse 80, 4056 Basel, Switzerland

Received: June 3, 2010; Revised Manuscript Received: August 5, 2010

The formation, stability, and dynamics of water filaments in disordered environments is investigated by using atomistic molecular dynamics simulations. It is found that in an alkyl-chain arrangement representative of that used in liquid chromatography, extended water filaments can form for up to 1 ns before they are destroyed again due to thermal fluctuations. The water dynamics in the disordered stationary phase is surprisingly intense with about 10^7 per alkyl chain per second of water molecules flowing in and out of the stationary phase. This is compatible with estimates based on Fick's law using a homogeneous solubility-diffusion model. The simulations also establish the existence of different types of water molecules as was predicted 30 years ago. From the current simulations they can be identified as (SiOH^-) surface-bound, interfacial, and bulk water molecules.

1. Introduction

Ordered water structures have been proposed to play a fundamental role in biological systems where they were implicated in transporting charge (protons).^{1–4} Examples for such “proton wires” include hydrogen-bonded chains in the photosynthetic reaction center of *Rhodobacter sphaeroides* where the chain extends from the interior of the protein to the cytoplasmic side,⁵ cytochrome *c* oxidase where chains of water molecules and amino acid side chains that can be protonated/deprotonated are found,^{6,7} or cytochrome *f* with a five-membered water chain extending from the interior heme group toward the outside of the protein.^{8,9} It has also been proposed that water assists proton transport through lipid bilayers even in the absence of specific channels.¹⁰ However, atomistic insight into the processes is difficult to gain in such systems as structure determination is in general not possible.

Alternatively, it has been found that a cell when placed in nonisotonic solution can shrink or swell, which indicates that the cell membrane is semipermeable and allows for exchange of water and/or ions.¹¹ The importance of water molecules in biological systems, primarily proteins, is undisputed and also well documented. It has also been shown that individual water molecules are explicitly involved in protein folding where it can play the role of a lubricant.^{12,13} On the other hand, directly investigating its role in cells and in membranes is more difficult. NMR and inelastic incoherent neutron scattering experiments of water interacting with planar membranes and tissue suggest that water inside cells behaves differently from bulk water.^{14,15}

Lipid hydration is of considerable importance in understanding the phase behavior of lipid/water systems and the forces between lipid bilayers. NMR experiments found that lipid head groups perturb the ordering and dynamics of interfacial water molecules compared to bulk water and suggested the existence of bulk, trapped, and up to three types of bound waters.¹⁶ By using infrared spectroscopy it is possible to probe the hydration sites of lipids. Alternatively, osmotic stress measurements have been used to investigate and differentiate between the role of water in binding to proteins and/or affecting its conformation

through changes in the activity of water.^{17,18} However, despite extensive work, relatively little structural data could be derived.¹⁹ This may be related to similar problems in structural biology where the assignment of infrared data to distinct structural states has only become possible recently through combination of experimental and computational approaches.^{20–22} The fundamental problem in such assignments, i.e., which structure corresponds to which spectroscopic feature, is the reorganization dynamics, which makes the investigation of structures by standard means (X-ray or NMR spectroscopy) difficult, if not impossible.

Water filaments in biological systems, as those mentioned above, all have clear functional roles. However, more or less ordered water networks have also been postulated or found in other condensed phase systems. One of them are chromatographic columns (see Figure 1) that consist of a stationary phase (solid support with alkyl chains attached) and a mobile phase with a solvent mixture (for details see section 2). Already 30 years ago, Scott and co-workers suggested that individual water molecules can bind to the $-\text{OH}$ groups of a silica surface and form a thermodynamically stable (fractional) monolayer.²³ These water molecules, thought to be present up to temperatures of around 650 °C, can serve as H-bond donors to additional water molecules that eventually form filaments. The morphology, stability, or mere existence of such filaments has, however, never been directly investigated. This is due to the heterogeneous and amorphous state of a chromatographic column. Owing to the great technological importance of chromatographic techniques, a more detailed understanding of water dynamics, energetics, and structuring in the stationary and the mobile phase seems desirable.

Here, we investigate the formation, stability, and morphology of water filaments using atomistic computer simulations by addressing the following specific questions: can ordered water structures form in dynamical, heterogeneous environments; how many water molecules are involved in water filaments; are these water molecules organized; and what is the influence of the solvent composition (cosolvent) on the formation and stability of water filaments? Classical molecular dynamics (MD) simula-

* To whom correspondence should be addressed at m.meuwly@unibas.ch.

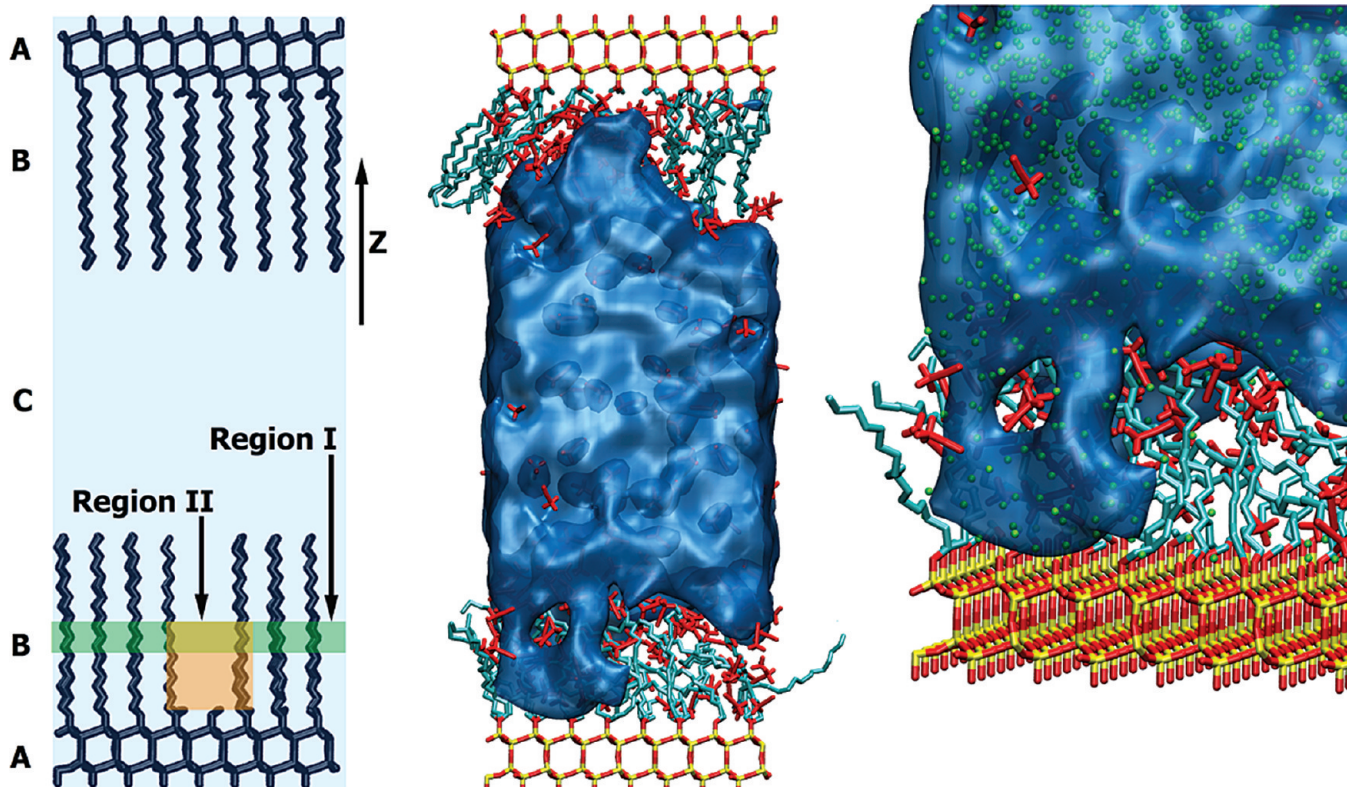


Figure 1. Water filament in the nonfunctionalized system with 20:80 ACN to water ratio. The left panel shows a schematic representation of the system together with definitions of the regions into which the system was divided: A, silica layer; B, alkyl chains; C, bulk phase. A and B form the stationary phase. The *z* direction is indicated by an arrow. The middle panel shows the entire system. To better visualize water filaments, water is represented by a volumetric map generated with the Situs program.⁴⁶ An example for a water filament is shown in the lower left corner of the system. The right panel shows the water filament and water molecules (green spheres represent oxygen atoms of water molecules) that are engaged in its formation. ACN molecules are red wire frames and hydrogen atoms of the alkyl chains (cyan) are not shown for clarity. The figure was prepared using the VMD software⁴⁷ from a snapshot taken at 16.78 ns of the MD simulation.

tions are ideal to study such questions as they allow us to follow the temporal evolution of complex systems on the atomistic level.

2. Computational Methods and Data Analysis

2.1. Chromatographic System. Figure 1 shows a schematic representation of the system together with a snapshot from MD simulations. The chromatographic system was described in detail previously.^{24,25} Briefly, the system consists of two silica layers on opposite sides of a rectangular parallelepiped. On every silica surface 24 alkyl chains replacing silanol groups were attached randomly to the silica which corresponds to a surface coverage of $2.65 \mu\text{mol}/\text{m}^2$. Additionally, 20 silanol groups on each silica layer were capped with $-\text{CH}_3$ and $-\text{OH}$ groups, respectively. Three different alkyl-chain functionalizations were studied: nonfunctionalized octadecane (CH_3 -terminated) and phenyl and nitrile functionalizations attached to the C17 atom of the octadecane chain. This system was solvated in pre-equilibrated solvent mixtures (acetonitrile (ACN)/water) with ratios of 20:80 and 50:50, respectively. The surface coverage, eluents, and ratios of their constituents were chosen so as to represent realistic reversed phase liquid chromatography (RPLC) experiments. Water was represented with the TIP3P model,²⁷ and for acetonitrile a previously validated all-atom model was employed.²⁴ In the following, labels such as c18.24.20.80 refer to systems with 24 nonfunctionalized (c18) alkyl chains and a ACN:water ratio of 20:80.

2.2. Molecular Dynamics Simulations. All MD simulations were carried out with the CHARMM²⁸ program, version c35b1,

and the CHARMM22 force field.²⁹ Force field parameters for the components of the system, i.e., silica layers, alkyl chains with and without the functional groups, and ACN, were previously determined.^{24,25}

Prior to the production simulations all systems were energy minimized using 5000 steps of steepest descent followed by heating from 50 to 300 K with temperature changing in increments of 10 K every 10 ps and equilibration for another 10 ps at 300 K. All production MD simulations were performed for 22 ns in the constant volume and constant temperature *NVT* ensemble at $T = 300$ K and with periodic boundary conditions (PBC). The time step in all simulations was 1 fs and SHAKE³⁰ was used to constrain all bonds involving hydrogen atoms. An atom-based cutoff was applied to calculate electrostatic and vdW interactions. Nonbonded interactions were truncated at a distance 8 Å between interacting atoms with a switching function. This approach has been previously validated in simulations with longer cutoffs.²⁴ All atoms except for the silanol groups in the silica layers were mobile throughout all MD simulations. Furthermore, the chromatographic model and simulation procedures employed here were validated in view of experimental data in previous work where it was found that the diffusion coefficient and reorientational time of an acridine molecule are correctly captured.²⁴ Additionally, earlier MD simulations²⁵ in the *NVT* ensemble, employing the same model, correctly predicted previously proposed microheterogeneity^{31–33} of ACN/water mixtures in RPLC interfaces.

2.3. Analysis of the Trajectories. For analyzing the MD trajectories, the simulation box was divided into a grid defined

by elements of size $1 \times 1 \times 1 \text{ \AA}$. This resulted in a grid with dimensions $37 \times 42 \times 98 \text{ \AA}$. The silica layers on both sides of the simulation box were covered by the grid, although their volume was not accessible to water or any other molecule in the system. The height of each of the silica layers is 9 grid elements along the z -axis. Additionally, the simulation box was divided into two regions: a stationary region (silica layers with the attached alkyl chains) and a bulk region (rest of the system). Then, water transport within the stationary phase and between the two phases was investigated.

Each of the stationary regions on both ends of the simulation box consists of 27 grid elements along the z -axis. Of these 27 elements, 9 correspond to the stationary silica support and 18 to the alkyl chains. This is consistent with a previous analysis by Braun et al.²⁵ in which the average length of alkyl chains in similar ACN/water mixtures was analyzed. As an example, the phenyl-functionalized alkyl chains with an average length of $17.9 \pm 0.8 \text{ \AA}$ correspond to 18 grid elements. To allow for direct comparison, the width of the alkyl-chain regions in all the systems studied was assigned to be equal to 18 grid elements. Thus, grid elements 1–27 and 72–98 along the z -axis represent the stationary phase, whereas grid elements 28–71 represent the bulk phase. Grid elements 10–27 and 72–89 represent the alkyl chains on the bottom and the top of the box, respectively.

The xyz-trajectory of individual water molecules is satisfactorily reproduced by a trajectory using grid coordinates (indices), which was verified by comparing traces of single water molecules from the MD simulations using their Cartesian coordinates and the respective grid coordinates.

Trajectory Volume. To analyze the mobility of water molecules, a trajectory volume V_t was introduced, which corresponds to the volume covered by each water molecule during an MD simulation. The volume is computed as the number of grid elements visited during the 16 ns of production simulation. Every visited grid element was counted once, irrespective of the number of times a water molecule occupied this grid element.

Exchange Dynamics. For detailed analysis of water exchange between the bulk and the stationary phases the alkyl-chain region of the stationary phase is divided into six layers with a height of three grid elements and an additional layer “seven” that represents the bulk phase. Depending on its initial position, every water molecule in the stationary phase was assigned to the corresponding layer. Subsequently, the number of water molecules that left the selected layer during the MD simulations and entered the other layers was counted. Counting was continued until a water molecule left the stationary phase and entered the bulk phase. In addition, the residence time for every water in each layer was measured.

Filament Detection. To describe dynamics of water in the stationary phase the flux of water molecules into this region was analyzed. To detect possible water filaments, water molecules that appeared in the middle of the height of the alkyl-chain region (region I depicted with green color in Figure 1) were counted. Region I represents a layer of thickness equal to 2 grid elements. The bottom and top region I consists of grid elements 17, 18 and 81, 82 along the z -axis, respectively. In x - and y -directions region I extends over the entire dimension of the system. Region I is particularly suited for such an analysis because it allows for efficient detection of possible water fluxes through the alkyl-chain region. The analysis of water fluxes in the regions close to the interface between the stationary and the bulk phase would result in detection of frequent bursts of water molecules from the bulk to the top of the stationary phase.

Most of such bursts do not form water filaments spanning the entire width of the alkyl-chain region. On the other hand, scanning regions close to the silica layers would result in primarily finding water molecules strongly bound to the surfaces. Though these water molecules can participate in formation of the filaments, they cannot be used to uniquely identify regions where the filaments are possibly formed.

Once water flux through region I is detected, more detailed analysis of water transport can be performed. For that purpose region II was introduced, which spans from the middle of the height of the alkyl-chain region to the silica surface along the z -axis as depicted schematically in the left-hand side panel of Figure 1. The x - and y -dimensions of region II were determined and defined as regions of high water fluxes in region I, as shown by the contours in Figures 2 and 3. For the 20:80 mixture with the nonfunctionalized chains, region II was defined from grid elements 5 to 20 along the x -axis, from 0 to 10 along the y -axis, and from 9 to 18 along the z -axis. For the 50:50 mixture with nonfunctionalized alkyl chains the region of interest included elements 13–23, 30–40, and 9–18 along the x -, y -, and z -axes, respectively. These areas in the xy -plane are shown as green rectangles in Figures 2 and 3.

3. Results

3.1. Equilibrium Dynamics in the Stationary Phase. To study the equilibrium dynamics of the solvent in the chromatographic system (Figure 1), the onset of equilibration for each of the systems (i.e., three different functionalizations, $-\text{CH}_3$, $-\text{CN}$, $-\text{NH}_2$, and two different eluent compositions for each of the functionalizations, 20:80 and 50:50 ACN to water ratio) was first determined. For the present investigation it is meaningful to characterize such a state by an approximately constant number of water molecules in the stationary and in the bulk phase. Analysis of the system after equilibration allows determining properties of the system that are not influenced by the relaxation of a nonequilibrium distribution.

Equilibration was quantified by considering the water flux between the stationary and the bulk phase. Figure 4 shows changes in the total number of water molecules in the stationary phase as well as water influx and efflux monitored relative to the first frame of the production MD simulations. Additionally, the water occupation of the silica layer is reported. Analysis of Figure 4 (red and green traces) reveals that particular molecules initially assigned to the stationary phase move to the bulk phase and vice versa. It is found that after ≈ 6 ns the average number of water molecules leaving or entering the stationary phase together with the total number of water molecules in this phase oscillates around a constant value. Thus, all further analysis is performed for 16 ns of simulation time, i.e., from 6 to 22 ns.

Figure 4 shows that systems with a different ACN to water ratio exhibit significantly different numbers of water molecules in the stationary phase. This is consistent with previous work²⁵ and can be attributed to the different distribution of the individual constituents of the eluent at the interface of the bulk and stationary phases. On the other hand, the numbers of water molecules directly interacting with the silica layers are similar in all the systems studied. Table 1 compares the average number $\langle N_{\text{silica}} \rangle$ of water molecules at a distance shorter than 2.4 \AA from any atom of the silica layers, which shows that most of these sites are occupied by water; i.e., the silica surface is “wet”. In the stationary phase, the total number of water molecules, N_{stat} , oscillates around fairly well-defined average values (Figure 4). However, at particular instances sudden and pronounced burst-like changes in N_{stat} can occur. Such fluctuations characterize

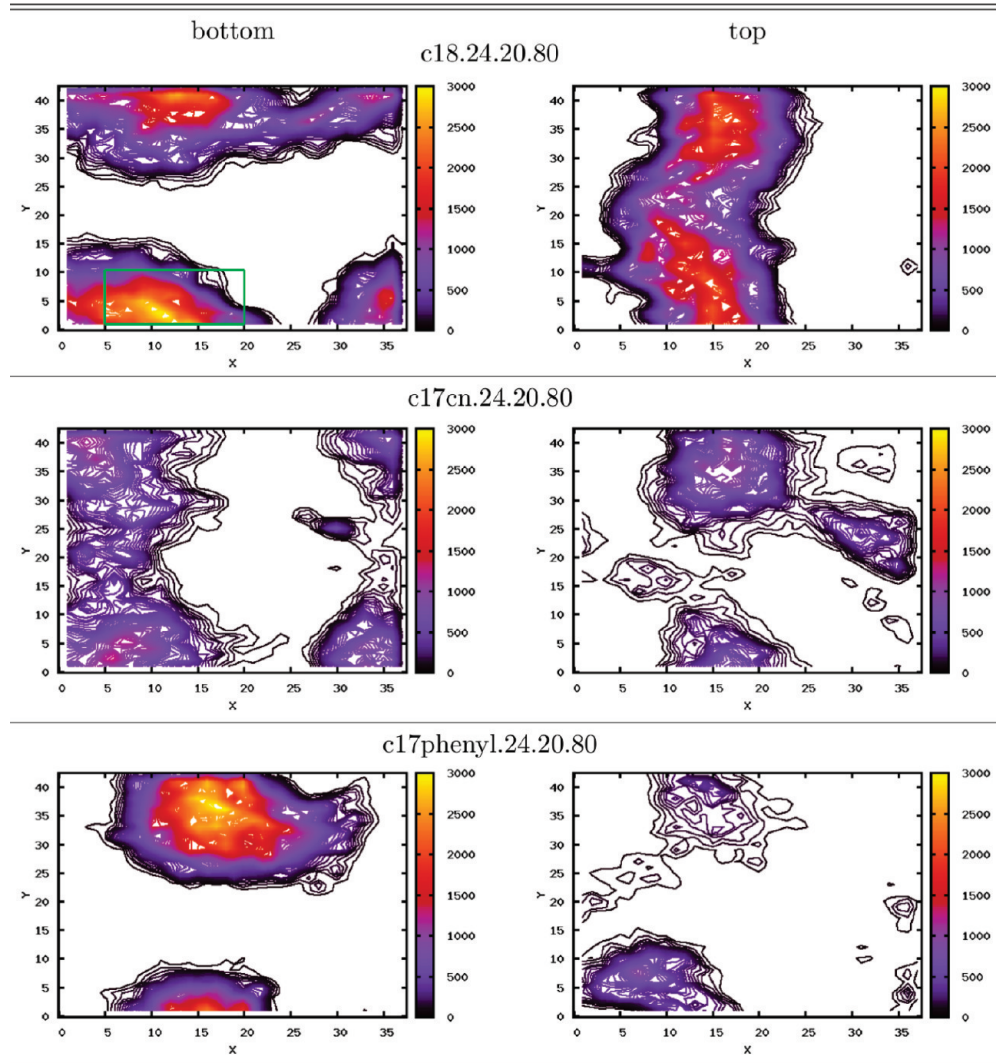


Figure 2. Sum of water molecules forming water filaments during 16 ns projected on the xy -plane of the grid (20:80 ACN to water ratio). The water molecules are in grid elements 17, 18 and 81, 82 along the z -axis (i.e., in the middle of the stationary phase). The green rectangle shows the xy -boundaries of region II.

water dynamics and are related to formation of water filaments connecting the bulk phase with the silica layer (see below). Figure 4 shows that fluctuations in N_{stat} (blue line) are correlated with fluctuations in the number of water molecules entering the stationary phase (green line).

3.2. Water Dynamics in the Stationary and Mobile Phases. Insets in Figure 5 present histograms obtained from the analysis of the trajectory volume V_t , which is proportional to the number of grid elements visited during a simulation (see section 2). The majority of water molecules contributes to large peaks at $V_t \approx 22\,000$ (20:80 ACN to water mixture) or $V_t \approx 19\,500$ (50:50 mixture). Water molecules in these two groups are highly mobile. On the other hand, about 30 ± 5 water molecules, depending on the system studied, are trapped in the stationary phase and lead to small peaks with trajectory volumes of $V_t \approx 0$. These peaks correspond to strongly immobilized water molecules that are H-bonded to the silica surface. Finally, there are several small peaks (individual water molecules) with $0 < V_t \leq 19\,000$. These correspond to water molecules that were initially located in the stationary phase and during the MD simulations diffused into the bulk phase where they remain or vice versa. It is interesting to note that although the simulation box for the 20:80 and 50:50 systems had the same physical dimensions, the accessed volume of the highly

mobile water molecules in the 50:50 system is significantly smaller than that for 20:80 (≈ 3000 which is about 14%). This can be explained by an increased ACN concentration in the stationary phase for the 50:50 system compared to the 20:80 system, which results in increased average alkyl-chain length in the 50:50 system, as was previously observed.²⁵

Figure 5 shows the relationship between V_t and the residence time of individual water molecules between the alkyl chains. The relationship between these two quantities is linear and suggests that V_t can be used as a measure for the residence time of water molecules between the alkyl chains. From the data in Figure 5 it was possible to identify and track water molecules covering different volumes V_t . Analysis of the individual trajectories allowed for distinguishing three groups of water molecules corresponding to different values of V_t . Group A consists of water molecules with $V_t < 2000$ and represents molecules that never leave the stationary phase, i.e., “trapped water”. Group B is characterized by $2000 \leq V_t \leq 18\,000$, which consists of waters that mostly occupy the bulk but also enter the alkyl-chain region and remain there for some time, i.e., “interfacial water”. Group C has $V_t > 18\,000$ and represents highly mobile water molecules that never enter the stationary phase, or enter it only briefly, and mostly remain in the bulk phase, i.e., “bulk water”. Results of the above analysis are

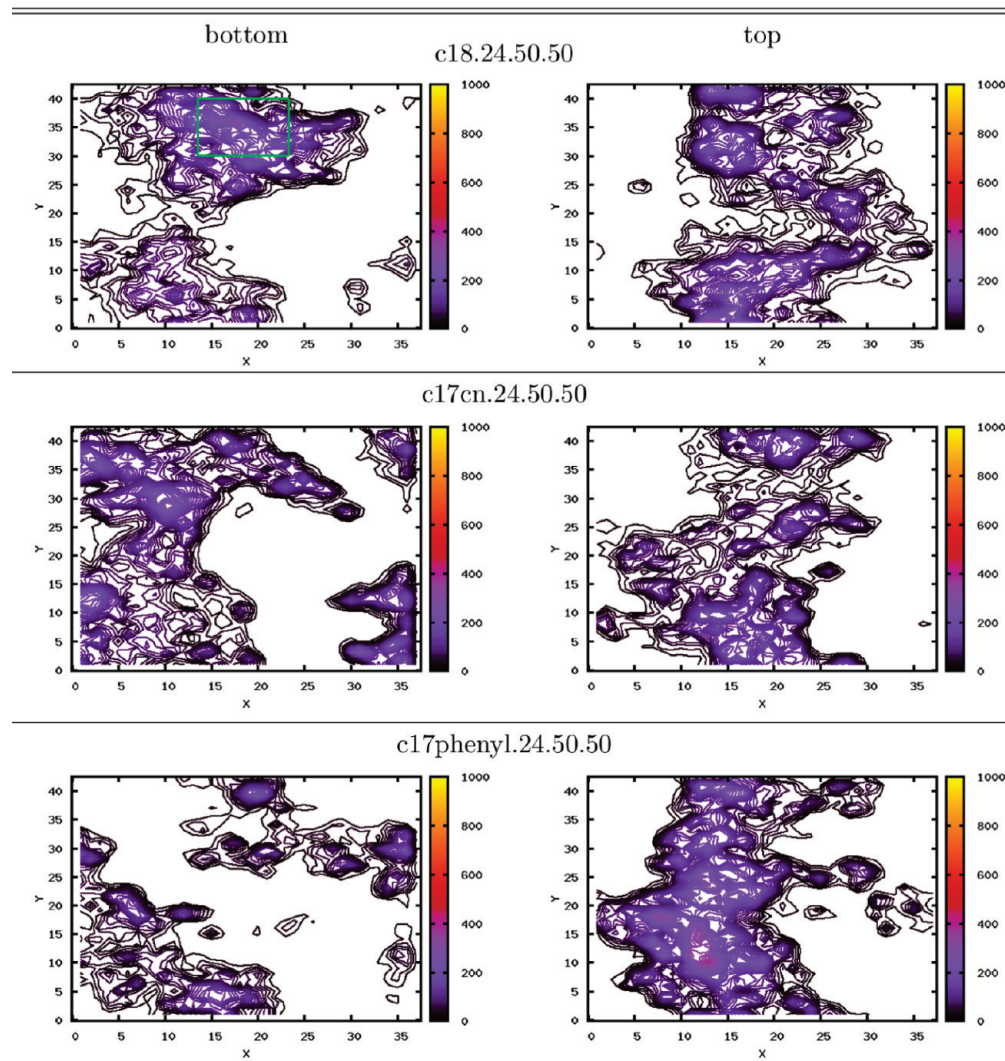


Figure 3. Sum of water molecules forming water filaments during 16 ns projected on the xy -plane of the grid (50:50 ACN to water ratio). The water molecules are in grid elements 17, 18 and 81, 82 along the z -axis (i.e., in the middle of the stationary phase). The green rectangle shows the xy -boundaries of region II.

summarized in Table 2, which reports the number of water molecules covering different trajectory volumes V_i . It is interesting that for the systems studied, the numbers from Table 1 are almost reproduced in column I of Table 2 in spite of the fact that thresholds in Table 2 for the trajectory volume are largely arbitrary. This correspondence validates the approach of using the trajectory volume as a measure of water molecule mobility and as a way to detect highly immobile water molecules.

In summary, equilibrium simulations allow us to broadly distinguish three different types of water molecules: trapped, interfacial, and bulk. They are characterized by different trajectory volumes covered during the MD simulations.

3.3. Vertical Water Dynamics in the Stationary Phase. The exchange of water molecules between the bulk and the stationary phase occurs along the z -axis of the system (Figure 1). To further characterize the exchange dynamics and the formation of water filaments in the stationary phase, the diffusion of water molecules along the z -axis was analyzed in more detail (see section 2).

Table 3 reports the number of water molecules initially located in a specific layer (indicated by bold font and *) along with the number of water molecules that left the initial layer and entered other layers of the stationary and the bulk phase. Results in the table refer to nonfunctionalized systems. For

c18.24.20.80 initially 56 water molecules are in layer 1. During the simulation 37 out of the 56 water molecules migrate to layer 2, 28 out of 37 from layer 2 enter layer 3, and finally 26 leave the stationary phase and migrate to the bulk. Similar analysis was carried out for all other layers as the initial layers. Additionally, the average residence times of water molecules in certain layers are reported. If a water molecule is initially in layer 1, its residence time in that layer is significantly longer than for the other layers. Moreover, some of them never leave the stationary phase, which is indicated by a difference of the initial number of water molecules in the first layer and the number of water molecules in layer 7 representing the bulk phase. This observation suggests that such water molecules are particularly strongly confined between alkyl chains, mostly due to the strong H-bond interaction with the silanol groups. If a water molecule is initially in layer 2, the sum of residence times in layers 1 and 2 is also outstanding, though shorter than if it is initially in layer 1. Similarly, for initial layer 3, the sum of residence times in layers 1, 2, and 3 is shorter than for the two aforementioned cases. If the water molecule is initially in layers 4, 5, or 6, the water molecule leaves the stationary phase and escapes to the bulk phase. Water molecules in layers 4–6 have the shortest residence times, which shows that they rapidly pass

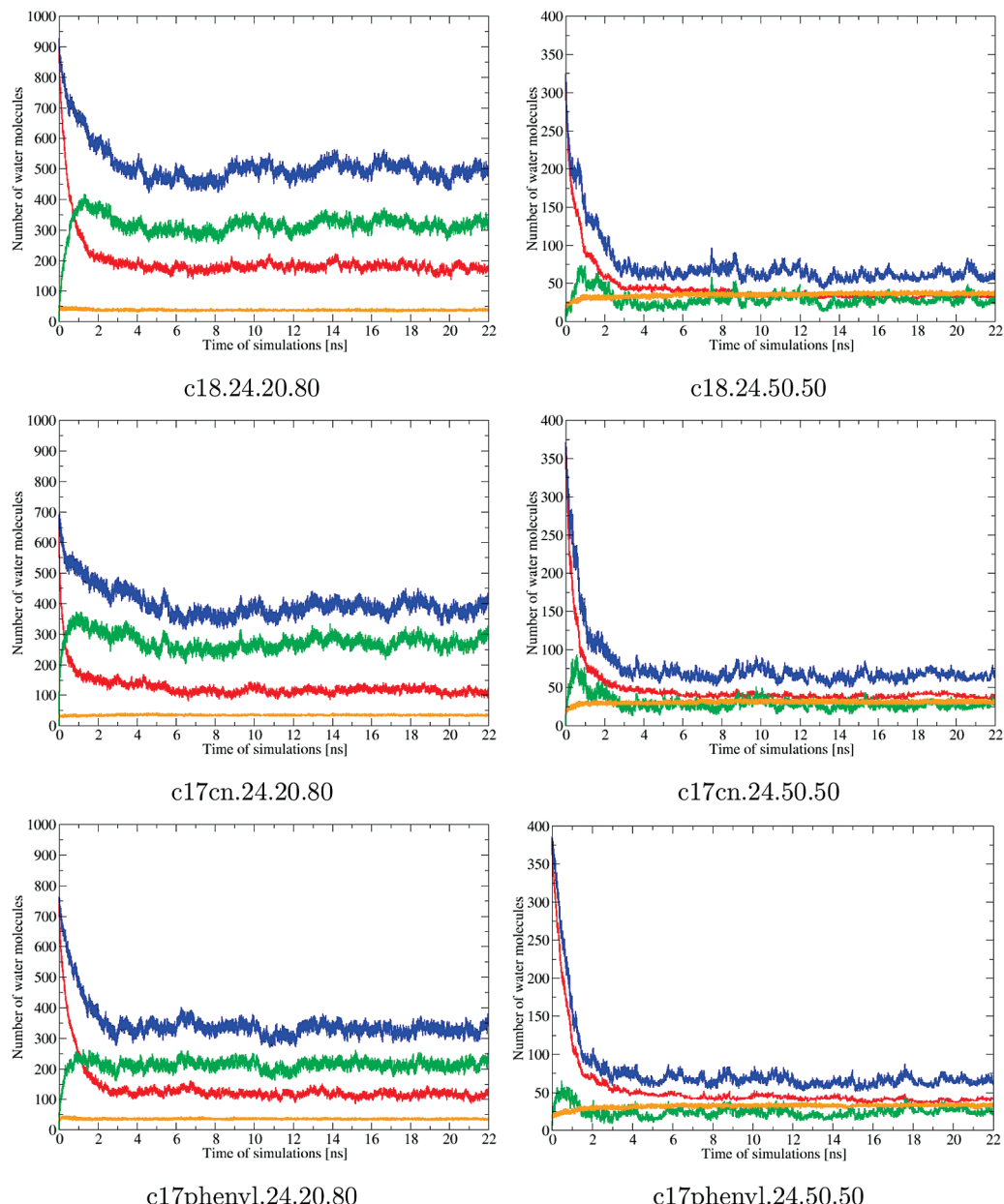


Figure 4. Inflow and outflow of water molecules from between alkyl chains measured with respect to the initial frame of the production MD simulations: red, outflow of water molecules from the stationary to the bulk phase; green, inflow of water molecules from the bulk to the stationary phase; blue, total number of water molecules in the stationary phase (identical to the sum of the red and green plots); orange, occupation of the hydroxyl groups on the silica layers.

TABLE 1: Average Number of Water Molecules Constantly Occupying the Silica Layers $\langle N^{\text{silica}} \rangle$ (Standard Deviation in Parentheses)

| system | $\langle N^{\text{silica}} \rangle$ |
|--------------------|-------------------------------------|
| c18.24.20.80 | 27 (1) |
| c18.24.50.50 | 35 (1) |
| c17cn.24.20.80 | 34 (1) |
| c17cn.24.50.50 | 31 (1) |
| c17phenyl.24.20.80 | 35 (1) |
| c17phenyl.24.50.50 | 32 (1) |

these layers. Similar results were obtained for the two functionalized systems studied in this work.

Only water molecules from layer 1 are sufficiently close to the silica surface to form strong H-bonds with the silanol groups. On the other hand, water molecules initially located in layers 3 and higher are weakly bound and can leave this region more readily than water molecules from layer 1.

The above analysis shows that once a particular water molecule approaches the region of the stationary phase that is within a distance of 3–6 Å from the silica surface, its dynamical properties change compared to those of water molecules outside of this region. This can be quantified by considering diffusion coefficients D (in units of (cm^2/s)), calculated from the mean square displacement (MSD),³⁴ for water molecules in different layers. For water molecules located initially in layer 1 the average diffusion constant is $D = 0.5 \times 10^{-5}$; for layers 2 and 3 $D = 1.5 \times 10^{-5}$; for layers 4–6 on average $D = 2.0 \times 10^{-5}$ and in the solvent mixture (bulk) also $D = 2.0 \times 10^{-5}$ compared with an experimentally measured value of 2.3×10^{-5} for pure water.³⁵

Again, typically three types of water molecules are found: trapped water molecules that reside mostly in layer 1 close to the silica surface, interfacial water molecules that diffuse in layers 1–3 with the possibility of leaving the stationary phase,

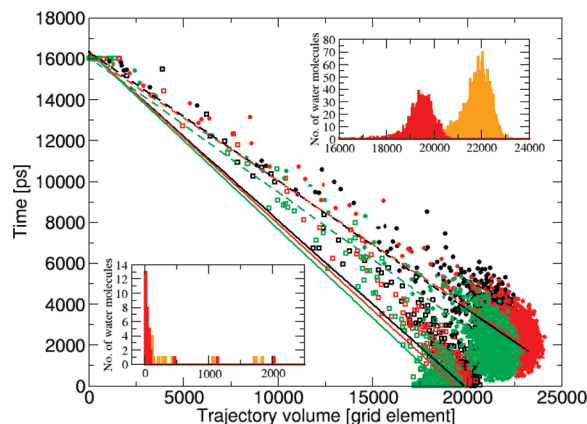


Figure 5. Comparison of the trajectory volume and the residence time of water molecules between alkyl chains. Full circles represent results for 20:80 ACN to water; empty squares are for a 50:50 ratio. Color code: nonfunctionalized chains (black), nitrile-functionalized chains (red), and phenyl-functionalized chains (green). Dashed lines are a linear regression to the data for the 20:80 systems, and continuous lines to that of the 50:50 systems. The inset in the lower left corner shows histograms of the volume trajectory for low-mobility water molecules and nonfunctionalized chains for both ACN to water ratios studied (20:80, orange; 50:50, red). The inset in the upper right corner reports histograms of the volume trajectory for highly mobile water molecules. The *x*-axis in all plots represents the trajectory volume with grid elements as a unit (see section 2 for definition of the trajectory volume).

TABLE 2: Number of Water Molecules with a Specific Trajectory Volume^a

| system | I ^b | II | III |
|--------------------|----------------|-----|------|
| c18.24.20.80 | 34 | 32 | 2769 |
| c17cn.24.20.80 | 27 | 25 | 2558 |
| c18phenyl.24.20.80 | 36 | 22 | 2537 |
| c18.24.50.50 | 30 | 44 | 1365 |
| c17cn.24.50.50 | 33 | 54 | 1447 |
| c18phenyl.24.50.50 | 36 | 164 | 1372 |

^a Three different groups of water molecules, differentiated by their trajectory volumes, can be distinguished (see Figure 5). ^b I, $V_t \leq 2000$; II, $2000 < V_t \leq 18\,000$; III, $V_t > 18\,000$.

and a third type, bulk water molecules, residing in the bulk phase and in layers 4–6 on top of the stationary phase.

TABLE 3: Number of Water Molecules in the Layers of the Stationary Phase and Their Average Residence Time for Nonfunctionalized 20:80 and 50:50 Systems^a

| | A | | B | | A | | B | | A | | B | | A | | B | | |
|--------------|----|---------|----|----|---------|----|----|--------|----|----|-------|----|-----|-------|----|-----|-------|
| | 1* | 2 | 3 | 4 | 5 | 6 | 7 | 8 | 9 | 10 | 11 | 12 | 13 | 14 | 15 | 16 | |
| c18.24.20.80 | 56 | 40571.0 | 1 | 10 | 7172.5 | 1 | 2 | 99.0 | 1 | 1 | 34.0 | 1 | 3 | 171.3 | 1 | 0 | 0.0 |
| 2 | 37 | 2403.7 | 2* | 14 | 1363.7 | 2 | 9 | 384.7 | 2 | 4 | 185.2 | 2 | 6 | 559.8 | 2 | 1 | 36.0 |
| 3 | 28 | 311.2 | 3 | 14 | 218.0 | 3* | 17 | 145.8 | 3 | 27 | 115.6 | 3 | 22 | 164.0 | 3 | 6 | 115.8 |
| 4 | 27 | 196.7 | 4 | 14 | 272.6 | 4 | 17 | 210.9 | 4* | 68 | 175.4 | 4 | 76 | 133.4 | 4 | 31 | 117.5 |
| 5 | 26 | 157.7 | 5 | 14 | 202.7 | 5 | 17 | 151.4 | 5 | 68 | 180.0 | 5* | 148 | 145.9 | 5 | 88 | 112.0 |
| 6 | 26 | 77.2 | 6 | 14 | 71.9 | 6 | 17 | 91.5 | 6 | 68 | 88.3 | 6 | 148 | 79.0 | 6* | 217 | 72.3 |
| 7 | 26 | nd | 7 | 14 | nd | 7 | 17 | nd | 7 | 68 | nd | 7 | 148 | nd | 7 | 217 | nd |
| c18.24.50.50 | | | | | | | | | | | | | | | | | |
| 1* | 44 | 45746.8 | 1 | 3 | 41780.0 | 1 | 4 | 2423.2 | 1 | 0 | 0.0 | 1 | 0 | 0.0 | 1 | 0 | 0.0 |
| 2 | 18 | 2781.4 | 2* | 3 | 1016.3 | 2 | 4 | 1817.5 | 2 | 0 | 0.0 | 2 | 0 | 0.0 | 2 | 0 | 0.0 |
| 3 | 17 | 657.5 | 3 | 2 | 220.0 | 3* | 4 | 673.0 | 3 | 2 | 39.0 | 3 | 0 | 0.0 | 3 | 0 | 0.0 |
| 4 | 17 | 388.6 | 4 | 1 | 239.0 | 4 | 4 | 305.2 | 4* | 2 | 182.0 | 4 | 1 | 120.0 | 4 | 0 | 0.0 |
| 5 | 17 | 275.6 | 5 | 1 | 298.0 | 5 | 4 | 131.2 | 5 | 2 | 321.0 | 5* | 2 | 108.5 | 5 | 0 | 0.0 |
| 6 | 17 | 102.1 | 6 | 1 | 48.0 | 6 | 4 | 128.8 | 6 | 2 | 113.5 | 6 | 2 | 53.0 | 6* | 3 | 57.0 |
| 7 | 16 | nd | 7 | 1 | nd | 7 | 4 | nd | 7 | 2 | nd | 7 | 2 | nd | 7 | 3 | nd |

^a A = number of water molecules, B = average residence time [fs], * = initial layer, nd = not determined.

TABLE 4: Sum of Water Molecules in Region I Calculated over Entire 16 ns of the Trajectory

| system | top ^a | bottom | total |
|--------------------|------------------|---------|-----------|
| c18.24.20.80 | 676 348 | 674 070 | 1 350 418 |
| c17cn.24.20.80 | 188 318 | 344 590 | 532 908 |
| c17phenyl.24.20.80 | 82 863 | 554 334 | 637 197 |
| c18.24.50.50 | 57 784 | 54 925 | 112 709 |
| c17cn.24.50.50 | 49 905 | 65 198 | 115 103 |
| c17phenyl.24.50.50 | 81 971 | 29 394 | 111 365 |

^a Top and bottom refer to region I in 81, 82 and 17, 18 grid elements along the *z*-axis, respectively.

3.4. Exchange Dynamics and Water Filaments. The observation of appreciable water flux across the interface and graphical analysis of the trajectories raises the interesting question whether stationary and ordered water structures can form in such a highly dynamical system. To identify water filaments, water flux through region I in Figure 1 was analyzed in more detail (see section 2) and the results are presented in Figures 2 and 3 as cumulative sums of the number of water molecules passing through region I. For all systems studied, the distribution of water molecules is strongly inhomogeneous and regions of particularly high water concentration can be found. The total number of water molecules across region I during 16 ns of MD simulations is summarized in Table 4.

For the 20:80 ACN to water mixture the largest number of water molecules is observed for the nonfunctionalized chains, while the lowest flux occurs for nitrile functionalization and the phenyl-substituted alkyl chain is intermediate. The nitrile-functionalized system exhibits the highest relative concentration of ACN in the stationary phase, whereas for nonfunctionalized chains the ACN concentration is the lowest.²⁵ Phenyl-substituted alkyl chains are between the two other systems in terms of ACN concentration in the stationary phase. Therefore, it is easier for water molecules to penetrate nonfunctionalized alkyl chains than substituted ones. Moreover, phenyl-functionalized alkyl chains can prevent water access to the stationary region by orienting the phenyl groups parallel to the silica surface. Comparing high- and low-water-containing systems shows that water concentration in the middle of the stationary phase is more pronounced for 20:80 than for 50:50 mixtures. This is due to the larger total number of water molecules in the 20:80 system. Thus, for high

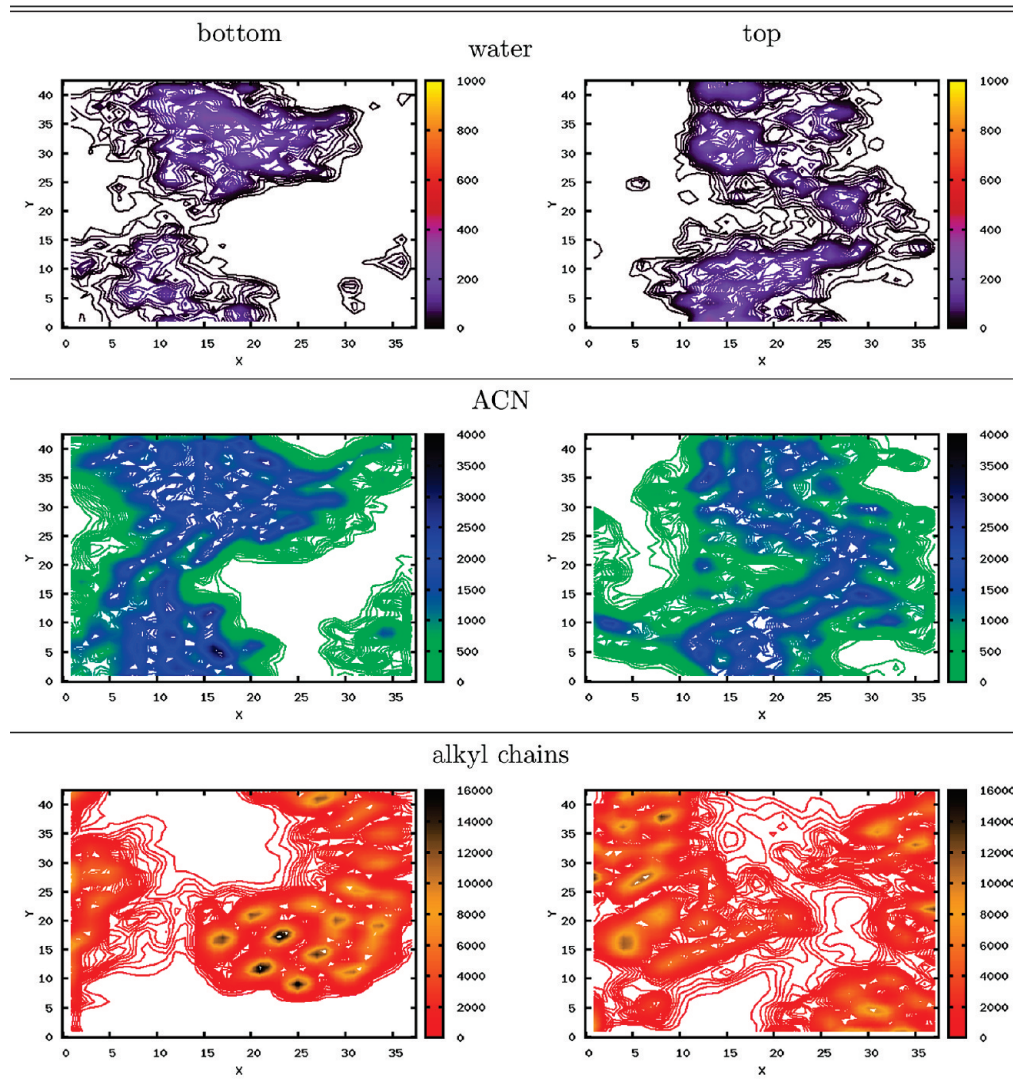


Figure 6. Distribution of water, ACN, and alkyl chains for the nonfunctionalized system with 50:50 ACN to water ratio projected onto the xy -surface of the grid. The distribution was calculated as a sum of water molecules (oxygen atoms) and alkyl chains (carbon atoms) present in region I (i.e., grid elements 17, 18 and 81, 82 along the z -axis, as shown in Figure 1). Due to its larger size, for ACN the nitrile carbon atom in grid elements 16–18 and 81–83 were followed for the analysis. “Bottom” and “top” correspond to analysis of grid elements 16–18 and 81–83, respectively.

water content the formation of connected water filaments is more probable than for low water concentration.

The dynamics of all components involved is strongly correlated. This is shown in Figure 6 as cumulative sums of each of the components of the system (water, ACN, and alkyl chain). The water distribution in the layers of the stationary phase considered proceeds in concert with motion of the ACN molecules and the alkyl chains. The distributions in Figure 6 show that water preferably enters regions of low alkyl-chain concentration. Furthermore, ACN molecules can facilitate penetration of the alkyl-chain region by water due to the hydrophilic and lipophilic properties of ACN. On one hand, ACN mixes well with water; on the other hand, its increased lipophilicity compared to that for water allows ACN to enter the alkyl-chain region.

The contours in Figures 2 and 3 reveal that there are regions in the xy -plane (green rectangles) that exhibit high water concentrations in region I. To detect water filament formation, water molecules in region II (see section 2) were analyzed. Results of this analysis for the nonfunctionalized alkyl chains in 20:80 and 50:50 ACN to water mixtures are presented in

Figure 7A,B, respectively, from which the average number of water molecules in region II and the average residence time for a single water molecule can be obtained.

The overall number of water molecules in region II over the entire simulation time (orange trace in Figure 7A,B) allows us to quantify the number of water molecules in a filament and to also establish maximal lifetimes of a filament. For the 20:80 nonfunctionalized system the average residence time of water is 0.14 ns with a maximal lifetime of 10.7 ns. The minimal occupancy of the volume element analyzed is 2, and the maximum is 37 water molecules. The average number of water molecules is 14 ± 5 . For the 50:50 system the average residence time is 0.7 ns with a maximum of 10.6 ns. Here, the minimal number of water molecules was 1 and maximally 11 water molecules occupied the region with an average of 4 ± 2 . For comparison, the same analysis was performed for region II spanning the entire xy -dimension. For the 20:80 system the average residence time is 0.4 ns with a maximum of 16 ns, which corresponds to the total simulation time. A minimal and maximal number of 27 and 84 water molecules, respectively, was found with an average of 49 ± 12 . For the 50:50 ACN to

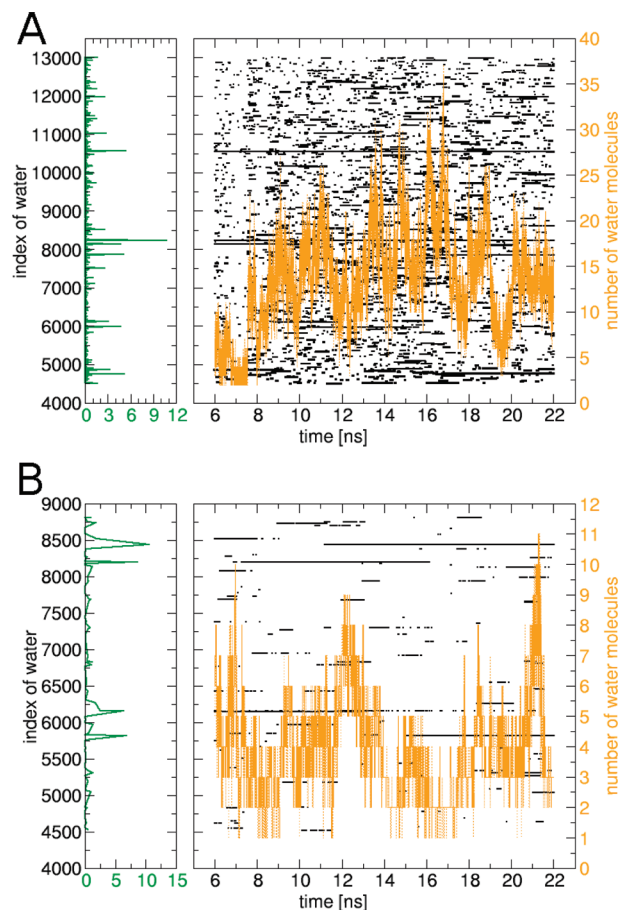


Figure 7. Flow of water in one of the filaments in the c18.24.20.80 (A) and c18.24.50.50 (B) systems analyzed in region II (see section 2 for definition): residence time of each water molecule in region II (left panels); time at which each water molecule was present in region II (right panels, black). The orange trace follows the sum of water molecules in region II over the entire simulation time.

water system the average residence time is 2.2 ns with the maximum at 16 ns. The minimal and maximal number of water molecules is 21 and 36 with an average of 27 ± 3 .

Typical lifetimes of such filaments in region II are on the order of 1 ns and form as bursts. Moreover, it is interesting to note that the total number of water molecules in the studied regions (orange curve) exhibits pronounced fluctuations, especially for the 20:80 system (see Figure 7A) where the number of water molecules can change from about 35 to 5 in less than 1 ns. It is found that the number of water molecules engaged in a filament can be up to 44% (37/84 for the 20:80 system) of the number of water molecules present in the entire cross section of the stationary phase at a given time along the trajectory.

4. Discussion and Conclusions

The present simulations establish the existence of ordered water filaments in hydrophobic environments with lifetimes on the order of 1 ns. Their formation has to be understood in the context of the motion of all other components of the system (stationary phase, cosolvent). The silanol surface is in general “wet”; i.e., water molecules are strongly bound to the $-\text{OH}$ groups of the stationary phase. Careful analysis of individual water molecules in the stationary phase leads to the conclusion that typically three types of water molecules can be distinguished. They differ in their lifetimes in particular regions of the stationary phase by about an order of magnitude (see

Table 3). This supports earlier suggestions²³ that postulated the existence of three different types of water molecules: type 1 is tightly bound to the silica surface where it remains throughout the simulation; type 2 diffuses between alkyl chains with relatively high mobility compared to the tightly bound water molecules; type 3 includes highly mobile water that exchanges between alkyl chains and the bulk solvent even at room temperature. It is worthwhile to mention that type 2 water molecules, although mobile, remain between the alkyl chains for most of the simulation time.

Compared with the original proposal,²³ type 1 water molecules correspond to Scott’s first solvation layer that leave the silica gel only at very high temperatures of about 650 °C (see Figure 10 in ref 23). Type 2 water molecules represent water molecules from the second layer of Scott’s model, which start detaching from the silica layer at 100 °C with complete loss at 120 °C. Finally, type 3 water molecules can represent the third layer from Scott’s observations. These are weakly bound water molecules that exchange with bulk solvent already at room temperature and up to 70 °C. Since occupation time is representative of the free energy of binding, we studied occupation times of water molecules located in the vicinity of the silica layer. The results collected in Table 3 together with the diffusion coefficients show that water molecules in layer 1 are significantly less mobile than other water molecules in the system and their residence time in layer 1 is much longer than residence times of water molecules in other layers of the stationary phase.

The present results also allow scrutinizing a previous proposal to explain the observed higher selectivity of RPLC to separate polycyclic aromatic hydrocarbons (PAH) when pure acetonitrile is used as an eluent instead of a 15:85 water to ACN mixture in the c18 stationary phases.³⁶ Wise and Sander proposed a “slot model” in which the bonded phase consists of narrow “slots” (space between alkyl chains) into which planar solute molecules can enter. In light of the present simulations this can be explained by the observation that for water/ACN mixtures as eluents, the water flux can fill the “slots” and thus competes with PAH molecules and reduces the selectivity of the column. To our knowledge no atomistic interpretation for this proposal has been available so far.

More recently, water structuring at interfaces has been investigated by using nonlinear optical techniques (vibrational sum frequency spectroscopy, VSFS) that capitalize on the selection rules for vibrational spectroscopy and make them sensitive to the water molecules at the interface but not in the bulk.^{37–41} At the CCl_4 /water interface the vibrational spectrum was interpreted in terms of water molecules that straddle the interface, those which are strongly interacting with bulk water and others that directly interact with CCl_4 .³⁹ At the water–air interface, different interpretations for the split spectrum in the 3200 and 3400 cm^{-1} region of the water stretching vibration have been put forward. One attributes these peaks to “ice-like” and “liquid-like” water species at the surface,^{37,41} whereas another interpretation finds the origin of the splitting in Fermi resonances due to couplings of vibrational modes.⁴⁰ Common to all these efforts is the difficulty that structural assignments of spectroscopic features in disordered environments is intrinsically problematic and greatly assisted by atomistic simulations.^{20–22} Finally, it may be difficult to use such methods to report on the structuring of the solvation layer beyond the direct interface because VSFS is most sensitive to water molecules directly at the interface.

It is also of interest to compare the number of water molecules transported across the chromatographic system studied here with estimates based on a simple homogeneous solubility-diffusion model.^{42–44} In the homogeneous solubility-diffusion model the flux of water is governed by Fick's equation $(1/F) \cdot (dn/dt) = -P\Delta c$, where n is a number of water molecules, t is time, P is the osmotic permeability coefficient of the membrane considered, and Δc is the water concentration gradient. Assuming a value of $P = 3 \times 10^{-3} \text{ cm/s}$ for the osmotic permeability of water,⁴⁵ the number of water molecules passing through 100 \AA^2 of a typical lipid membrane is about 9.6×10^5 water molecules per second. With an average area for a lipid chain in the lipid bilayer of 30 \AA^2 , the flux of water amounts to 3.2×10^5 molecules per lipid chain per second.⁴⁵

Results from Figure 7B allow us to estimate water permeability through the alkyl-chain region. For nonfunctionalized alkyl chains and a 50:50 ACN to water mixture, on average 3.2 water molecules per 16 ns per 100 \AA^2 are transported through the alkyl-chain region (high-density region). With an average area for a single alkyl chain of 63 \AA^2 this leads to a flux of $\approx 10^8$ water molecules per chain per second. In addition, it is possible to calculate the water flux through the entire area of the stationary phase. Considering the entire area of the simulated system the amount of water transported reduces by about an order of magnitude ($\approx 10^7$).

In conclusion, extensive atomistic simulations of a chromatographic system have shown that water plays a potentially important role in the physical chemistry of reversed phase liquid chromatography. Water filaments, which can form and melt several times during a particular simulation, with lifetimes of 1 ns extending over the entire width of the disordered stationary phase ($10\text{--}12 \text{ \AA}$) were identified. Two previously discussed and experimentally relevant scenarios, (a) three different types of water molecules involved in the hydration of the silica layer and the stationary phase and (b) the “slot model”, can be rationalized at an atomistic level, on the basis of the current simulations. Finally, the amount of water transported in and out of the system is in qualitative agreement with thermodynamic models based on Fick's law.

Acknowledgment. We gratefully acknowledge financial support from the Swiss National Science Foundation through grant 200021-121806. We thank Prof. J. Seelig (Biozentrum, University of Basel) for insightful discussions. A movie showing the formation and destruction of a filament from the present MD simulations is available from <http://www.chemie.unibas.ch/~meuwly/water.dyna.avi>.

References and Notes

- Nagle, J.; Morowitz, H. *Proc. Natl. Acad. Sci. U.S.A.* **1978**, *75*, 298.
- Humphrey, W.; Lu, H.; Logunov, I.; Werner, H.-J.; Schulten, K. *Biophys. J.* **1998**, *75*, 1689.
- Lanyi, J. *J. Biol. Chem.* **1997**, *272*, 31209.
- Baudry, J.; Crouzy, S.; Roux, B.; Smith, J. *Biophys. J.* **1999**, *76*, 1909.
- Tandori, J.; Sebban, P.; Michel, H.; Baciou, L. *Biochem.* **1999**, *38*, 13179.
- Michel, H. *Proc. Natl. Acad. Sci. U.S.A.* **1998**, *95*, 12819.
- Gennis, R. *Proc. Natl. Acad. Sci. U.S.A.* **1998**, *95*, 12747.
- Ponomarev, M.; Cramer, W. *Biochem.* **1998**, *37*, 17199.
- Sainz, G.; Carrell, C. J.; Ponomarev, M. V.; Soriano, G. M.; Cramer, W. A.; Smith, J. L. *Biochemistry* **2000**, *39*, 9164.
- Gensure, R.; Zeidel, M.; Hill, W. *Biochem. J.* **2006**, *398*, 485.
- Fettiplace, R.; Haydon, D. *Physiol. Rev.* **1980**, *60*, 510.
- Papoian, G. A.; Ulander, J.; Eastwood, M. P.; Luthey-Schulten, Z.; Wolynes, P. G. *Proc. Natl. Acad. Sci. U.S.A.* **2004**, *101*, 3352.
- Bolhuis, P. *Biophys. J.* **2005**, *88*, 50.
- Ruffle, S.; Michalarias, I.; Li, J. C.; Ford, R. *J. Am. Chem. Soc.* **2002**, *124*, 565.
- Garcia-Martin, M.; Ballesteros, P.; Cerdan, S. *Prog. Nucl. Magn. Reson. Spectrosc.* **2001**, *39*, 41.
- Finer, E.; Darke, A. *Chem. Phys. Lipids* **1974**, *12*, 1.
- Colombo, M. F.; Rau, D. C.; Parsegian, V. A. *Science* **1992**, *256*, 655.
- Parsegian, V. A.; Rand, R. P.; Rau, D. C. *Proc. Natl. Acad. Sci. U.S.A.* **2000**, *97*, 3987.
- Binder, H. *Eur. Biophys. J.* **2007**, *36*, 265.
- Plattner, N.; Meuwly, M. *Biophys. J.* **2008**, *94*, 2505.
- Lutz, S.; Nienhaus, K.; Nienhaus, G.; Meuwly, M. *J. Phys. Chem. B* **2009**, *113*, 15334.
- Nienhaus, K.; Lutz, S.; Meuwly, M.; Nienhaus, G. *ChemPhysChem* **2009**, *11*, 119.
- Scott, R. *Faraday Symp. Chem. Soc.* **1980**, *15*, 49.
- Fouqueau, A.; Meuwly, M.; Bemish, R. *J. Phys. Chem. B* **2007**, *111*, 10208.
- Braun, J.; Fouqueau, A.; Bemish, R.; Meuwly, M. *Phys. Chem. Chem. Phys.* **2008**, *10*, 4765.
- Sentell, K. B.; Dorsey, J. G. *J. Chromatogr. A* **1989**, *4610*, 193.
- Jorgensen, W.; Chandrasekhar, J.; Madura, J.; Impey, R.; Klein, M. *J. Chem. Phys.* **1983**, *79*, 926.
- Brooks, B. R.; Bruccoleri, R. E.; Olafson, B. D.; States, D. J.; Swaminathan, S.; Karplus, M. *J. Comput. Chem.* **1983**, *4*, 187.
- MacKerell, A. D., Jr.; Bashford, D.; Bellott, M.; Dunbrack, R. L., Jr.; Evanscek, J. D.; Field, M. J.; Fischer, S.; Gao, J.; Guo, H.; Ha, S.; Joseph-McCarthy, D.; Kuchnir, L.; Kuczera, K.; Lau, F. T. K.; Mattos, C.; Michnick, S.; Ngo, T.; Nguyen, D. T.; Prodhom, B.; Reiher, W. E., III; Roux, B.; Schlenkrich, M.; Smith, J. C.; Stote, R.; Straub, J.; Watanabe, M.; Wiorkiewicz-Kuczera, J.; Yin, D.; Karplus, M. *J. Phys. Chem. B* **1998**, *102*, 3586.
- Ryckaert, J. P.; Ciccotti, G.; Berendsen, H. *J. Comput. Phys.* **1977**, *23*, 327.
- Kovacs, H.; Laaksonen, A. *J. Am. Chem. Soc.* **1991**, *113*, 5596.
- Mountain, R. D. *J. Phys. Chem. A* **1999**, *103*, 10744.
- Reimers, J. R.; Hall, L. E. *J. Am. Chem. Soc.* **1999**, *121*, 3730.
- Allen, M. P.; Tildesley, D. J. *Computer simulation of liquids*; Clarendon Press: New York, 1989.
- Price, W. S.; Ide, H.; Arata, Y. *J. Phys. Chem. A* **1999**, *103*, 448.
- Wise, S.; Sander, L. *J. High Res. Chromatogr.* **1985**, *8*, 248.
- Du, Q.; Superfine, R.; Freysz, E.; Shen, Y. R. *Phys. Rev. Lett.* **1993**, *70*, 2313.
- Gragson, D. E.; Richmond, G. L. *J. Am. Chem. Soc.* **1998**, *120*, 366.
- Scatena, L. F.; Brown, M. G.; Richmond, G. L. *Science* **2001**, *292*, 908.
- Sovago, M.; Vartiainen, E.; Bonn, M. *J. Chem. Phys.* **2009**, *131*, 161107.
- Zhang, L.; Singh, S.; Tian, C.; Shen, Y. R.; Wu, Y.; Shannon, M. A.; Brinker, C. J. *J. Chem. Phys.* **2009**, *130*, 154702.
- Traeuble, H. *J. Membr. Biol.* **1971**, *4*, 193.
- Mathai, J.; Tristram-Nagle, S.; Nagle, J.; Zeidel, M. *J. Gen. Physiol.* **2007**, *131*, 69.
- Nagle, J.; Mathai, J.; Zeidel, M.; Tristram-Nagle, S. *J. Gen. Physiol.* **2007**, *131*, 77.
- Seelig, J. Private communication, Biozentrum, University of Basel, 2009.
- Wriggers, W.; Milligan, R. A.; McCammon, J. A. *J. Struct. Biol.* **1999**, *125*, 185.
- Humphrey, W.; Dalke, A.; Schulten, K. *J. Mol. Graph.* **1996**, *14*, 33.